Analytical and experimental study on dissolved pollutant wash-off over impervious surfaces

Yang Xiao[1], Taotao Zhang[1], Lei Wang[1], Dongfang Liang[2], Xingwu Xu[3]

1 College of Water Conservancy and Hydropower Engineering, Hohai University, Nanjing 210098, China

2 Department of Engineering, University of Cambridge, Cambridge CB2 1PZ, UK

3 Nanjing Sancha River Estuary Gate Administration, Nanjing 210036, China

Running head: Pollutant wash-off over impervious surfaces

Keywords: Dissolved pollutant; Urban runoff; Rainfall simulation; Diffuse pollution; Pollutant wash-off.

Abstract

Non-point source pollution in the impervious surface of city, which including dissolved and particulate pollutants, is a significant source of water pollution. Simple first-order decay models can generally simulate the cumulative wash-off process of the particulate pollutants. There is inadequate knowledge as to whether or not they are suitable for dissolved pollutants. This study presents a mathematical wash-off model for dissolved pollutants, which combines analytical equations for overland flows and the exponential equation for the pollutant wash-off. A series of laboratory experiments have been conducted to verify this wash-off model. It shows that the pollutant concentration and pollutant transport rate can be predicted well by the newly-developed equations. It is found that the pollutant concentration monotonically decreases to zero as the accumulated pollutants are washed off, while the pollutant transport rate first increases to the maximum value and then decreases to zero. The maximum pollutant transport rate is found to increase with the decrease of the arrival time of the maximum value. The difference between the simplified exponential model and the amended wash-off equation depends on the initial residual percentage (P_c), but the present equation generally provides a more accurate representation of the wash-off process of dissolved pollutants.

1. Introduction

Non-point source (NPS) pollution from urban storm runoff has been studied intensively since it can give rise to a series of serious environmental consequences and cause great economic losses (Yao et al., 2016). Ongoing urbanization and associated increases in impervious surface areas are likely to exacerbate the problem (Wang et al., 2013). It is widely accepted that pollutants originated from urban impervious surfaces contribute to the serious deterioration of the receiving water quality (Brezonik and Stadelmann, 2002; Hou, 2013; Lee and Bang, 2000; Vaze and Chiew, 2002). Therefore, it is essential to establish an appropriate wash-off model to understand the pollutant transport processes and design pollution mitigation strategies.

A number of researchers relied on a first-order decay model to interoperate the observations. The exponential wash-off equation proposed by Metcalf and Eddy Inc (1971) adopts the assumption that the rate of pollutant wash off from an impervious surface is proportional to the amount of surface pollutant presently available and the rate of storm-water runoff. Sartor and Boyd (1972) suggested that the wash-off can indeed be best replicated using the exponential equation. They also found that wash-off of particulate matter varies with the particle size distribution and presented different wash-off coefficients for different particle sizes. Egodawatta et al. (2007, 2009) applied such a model to pollutant wash-off on road and roof surfaces, but the dependence of the wash-off coefficient on particle sizes was not shown. Egodawatta et al. (2007, 2009) noted that a rainfall event has the capacity (depending on rainfall

intensity) to mobilize only a fraction of pollutants on the surface. Through these studies, researchers have gained a generally good understanding of the wash-off processes on road and roof surfaces. The wash-off model has been widely applied and verified (Charbeneau and Barrett, 1998; Deletic et al., 2000; Irish et al., 1998; Kim et al., 2005; Osuch-Pajdzińska and Zawilski, 1998).

The pollutant wash-off process over the ground surface is closely related to the runoff process. The accurate characterization of the overland flow process is key to predicting the transport of pollutants. However, many previous studies only focus on the cumulative wash-off process of pollutants but overlook the detailed runoff process. For a constant rainfall event, previous studies simply equate the rate of storm-water runoff per unit area to the rainfall intensity when applying the exponential wash-off model. Obviously, such a treatment is inappropriate at the initial rising stage of the runoff process. The initial part of the surface water runoff is associated with the first flush, which generates disproportionately high concentration of pollutants and thus rapid degradation of water quality during the rising limb of the runoff hydrograph. In addition, there have been limited studies (Xiao et al., 2016) to investigate the detailed mechanism of the transient processes of the pollutant concentration and the pollutant transport rate overall a small-scale uniform-slope surface. The wash-off equation may describe the process at a small catchment, but it cannot explain the pollutant concentration and pollutant transport rate runoff processes at a large catchment scale with multiple sources and transport rates. Xiao et al. (2016) suggested that the pollutant concentration and pollutant transport rate should be related to the rainfall

intensity, surface roughness, bed slope, catchment dimensions and initial amount of pollutant on the surface.

Furthermore, most existing studies focused on the particulate matter with the general assumption that most of stormwater-generated pollutants are adsorbed to solid particles (Sartor and Boyd, 1972; Sheng et al., 2008). However, stormwater-borne pollutants can also be in dissolved as well as particulate phases. There is inadequate knowledge as to whether or not the exponential wash-off model can be applied to dissolved pollutants. The difference in the transport of dissolved and particulate pollutants can be large, due to their different physical-chemical properties. Sheng et al. (2008) noted that the difference between dissolved and particulate pollutants has rarely been recognized for urban watersheds. Particulate pollutants are commonly regarded as the primary pollutant source in the urban environment, but the contribution from dissolved pollutants can be significant (Sansalone et al., 1996; Miguntanna et al., 2013). Goonetilleke et al. (2005) suggested that targeting particulate pollutants alone may not be effective in stormwater treatment.

The objective of this paper is to develop and test a mathematical wash-off model that better describes the transport of dissolved pollutants. To do this, an empirical wash-off model which combines the analytical solution of overland flow and the exponential wash-off equation has been developed to predict the pollutant concentration and pollutant transport rate. Next, a series of laboratory experiments, involving different rainfall intensities, surface roughness, bed slopes and initial amount of pollutants on the ground, have been conducted using rainfall simulators and

uniform-sloped idealized catchments to verify the amended wash-off model.

2. Mathematical model

Pollutant wash-off from an impervious surface is commonly modelled by an exponential equation proposed by Metcalf and Eddy Inc (1971):

$$W_t = W_0\left(1 - e^{-kV_t}\right) \quad (1)$$

where W_t is the amount of material having been removed in time t (kg); W_0 is the initial mass of the material on the surface (kg); k is the wash-off coefficient (m^{-1}); t is time (s); and V_t is the cumulative runoff depth since the start of rainfall (mm) that can be calculated by:

$$V_t = \int_0^t r\,dt \quad (2)$$

where $r = Q_t / A$ is the rate of storm-water runoff per unit area (m/s); Q_t is the runoff rate at time t, with the units of m^3/s; and A is the area of watershed, with the units of m^2.

For an unceasing constant rainfall event, the hydrograph displayed an initial rising limb, followed by a constant flow discharge which is equal to the rainfall input, i.e., as described by the rational formula. At the initial rising runoff process, r is smaller than I (the rainfall intensity, with the units of m/s). Only at the plateaued stage of the rainfall runoff, r is equal to I. As mentioned before, some previous studies simply equate the rate of storm-water runoff per unit area to the rainfall intensity during the entire rainfall runoff process when applying the above exponential wash-off model. If we adopt such a crude approximation, however, it will result in a contradiction. If $r = I$, Eq. (1) can be expressed as:

$$W_t = W_0\left(1 - e^{-kIt}\right) \quad (3)$$

Taking the derivative of Eq. (3) with respect to time, we can obtain the formulation of the pollutant transport rate:

$$M_t = \frac{dW_t}{dt} = W_0 kIe^{-kIt} \quad (4)$$

This pollutant flow rate can also be calculated using the following equation (Kim et al., 2005).

$$M_t = C_t Q_t \quad (5)$$

where C_t is the pollutant concentration at time t.

From Eq. (4), we can conclude that M_t is maximum at $t = 0$, and then gradually decreases to zero. However, the runoff rate should be zero when the water flow rate is zero. According to Eq. (5), the value of M_0 should be zero rather than a maximum, as $Q_0 = 0$.

The transport of pollutant is closely related to the overland flow process. Thus, the accurate quantification of the overland flow process is key to predicting the transport of pollutants. Numerous studies have developed numerical models to simulate the one-dimensional overland flows over a rectangular catchment (Liang et al., 2015; Gottardi and Venutelli, 1993, 2008; Jaber and Mohtar, 2003), and the results show that these models match well with the analytical solution of a kinematic wave model in idealized situations (Stephenson and Meadows, 1986). The analytical solution can be described as:

$$t_c = \left[L / \left(\alpha I^{m-1}\right)\right]^{1/m} \quad (6)$$

$$q_t = \alpha (h)^m = \alpha (It)^m \quad , \quad \mathbf{0} \le t \le t_c \tag{7}$$

$$q_t = \alpha (h)^m = \alpha (It_c)^m = LI \quad , \quad t_c \le t \le T \tag{8}$$

$$q_t = LI - I^m \alpha^{1/m} q_t^{1-1/m} (t - T) \quad , \quad T \le t \tag{9}$$

$$Q_t = q_t B \tag{10}$$

where t_c is the time of concentration (s); T is the rainfall duration (s); L is the length of the watershed (m); B is the width of the watershed (m); q_t is the unit width flow rate (m^2/s); h is the water depth (m); α can be defined as overcurrent capability coefficient ($m^{1/3}/s$); m is a dimensionless water depth index. The two coefficients, α and m, in the above expression can be derived using the Manning equation:

$$\alpha = S_0^{1/2} / n; \; m = \mathbf{5/3} \tag{11}$$

with n being the Manning roughness coefficient ($m^{-1/3}s$) and S_0 being the bed slope.

Taking the derivative of Eq. (1) with respect to the cumulative runoff volume, we can acquire the pollutant concentration C_t in the rainfall-runoff event over the impervious surface of area A:

$$C_t = \frac{\mathbf{1}}{A} \frac{dW_t}{dV_t} = \frac{W_0 k}{A} e^{-kV_t} = C_0 e^{-kV_t} \tag{12}$$

where C_0 is the initial concentration in mg/L.

For a constant rainfall event over an idealized catchment, we can acquire the formulation of pollutant concentration and pollutant transport rate at different stages through the manipulation of the above equations.

Stage 1 is when $\mathbf{0} \le t \le t_c$. Combining Eqs. (2), (7), (10), (11), and (12), we

obtain the formulation of C_t:

$$C_t = C_0 e^{-\frac{3}{8}k\alpha L^{-1} I^{5/3} t^{8/3}} \tag{13}$$

Combining Eqs. (5), (7), (10), (11) and (13), we obtain the formulation of M_t:

$$M_t = \alpha B C_0 \left(It\right)^{\frac{5}{3}} e^{-\frac{3}{8}k\alpha L^{-1} I^{5/3} t^{8/3}} \tag{14}$$

Integrating Eq. (14) over time, we obtain:

$$W_t = \int_0^t M_t dt = \int_0^t \alpha B C_0 \left(It\right)^{\frac{5}{3}} e^{-\frac{3}{8}k\alpha L^{-1} I^{5/3} t^{8/3}} dt = W_0 - W_0 e^{-\frac{3}{8}k\alpha L^{-1} I^{5/3} t^{8/3}} \tag{15}$$

We define $P_t = e^{-\frac{3}{8}k\alpha L^{-1} I^{5/3} t^{8/3}}$, so Eq. (15) can be written as follows:

$$W_t = W_0 \left(1 - P_t\right) \tag{16}$$

From Eq. (16), we can conclude that P_t represents the percentage of pollutants remaining on the watershed at time t. We can obtain the value of P_t at $t = t_c$ and define it as initial residual percentage (P_c).

$$P_c = e^{-\frac{3}{8}k\alpha L^{-1} I^{5/3} t_c^{8/3}} = e^{-\frac{3}{8}k(LI/\alpha)^{3/5}} \tag{17}$$

Stage 2 corresponds to $t_c \le t \le T$. At this stage, the runoff rate is a constant AI. V_t can be calculated by Eq. (18) as:

$$V_t = \frac{1}{A}\int_0^t Q_t dt = \frac{1}{A}\int_0^{t_c} Q_t dt + \frac{1}{A}\int_{t_c}^t Q_t dt = \frac{3}{8}\left(LI / \alpha\right)^{3/5} + I\left(t - t_c\right) \tag{18}$$

Combining Eqs. (12) and (18), we obtain the formulation of C_t:

$$C_t = C_0 e^{-\frac{3}{8}k(LI/\alpha)^{3/5} - kI(t-t_c)} = C_0 P_c e^{-kI(t-t_c)} \tag{19}$$

Combining Eqs. (5) , (8), (10)and (19), we obtain the formulation of M_t:

$$M_t = AIC_0 P_c e^{-kI(t-t_c)} \tag{20}$$

Integrating Eq. (20) over time, we obtain:

$$W_t = W_{t_c} + \int_{t_c}^t M_t dt = W_0 \left(1 - P_c e^{-kI(t-t_c)}\right) \tag{21}$$

In the following study, we only consider the condition that the rainfall duration is

sufficiently long such that there is little pollutant remaining on the watershed after the rainfall stops. Hence, the pollutant washed off after the rainfall has stopped is neglected.

3. Laboratory experiments

In this study, a series of laboratory experiments have been conducted to investigate various combinations of influencing factors. The experimental set-up is shown in Photographs (a) and (b) and in Fig. 1, which mainly consists of a small-scale catchment beneath a rainfall simulation system. A V-shaped flushing board is applied in this rainfall simulation system to guarantee the constant rainfall intensity. The V-shaped flashing board remains in an 'off' state until the steady rainfall state is achieved. Water nozzles are located 17 m above the model catchment. The rainfall intensity ranges from 20 mm/h to 200 mm/h, with the rainfall uniformity of over 0.9 over an area of 15.6 m in length and 12.6 m in width. The rainfall non-uniformity mainly occurs at the boundaries, which can be largely eliminated by placing the catchment at the center of the hall. The catchment consisted of two wooden boards (2.96 m length, 1.4 m width and 0.02 m thick) sit in a steel flume that allows the angle of the boards to be adjusted via a hydraulic system, as shown in Fig. 1. The main reasons for choosing the wooden boards are: (a) they are light and easy to handle; (b) they are not easy to be deformed for high strength; and (c) their surface can be treated easily. Three short walls with the height of 4 cm are fixed on three sides of each board so that water can only leave the idealized catchment at the downstream end. The

boards are identical with the exception of surface roughness. Hence, one is referred to as the S-board (smooth) and the other is the R-board (rough), with the exact roughness values determined later on according to the experimental runoff results. There are numerous tiny holes at the bottom of the flume to allow rainwater landing on the gap between the flume and board (defined as gap flow) to freely drain off.

In this study, the slope is set at 1°, 2° and 5°, respectively. Three constant rainfall intensities are tested according to the optimal operation range of the rainfall simulators, which are 40 mm/h, 80 mm/h, and 120 mm/h. Each rainfall lasted for 29 minutes. Similar to Deng et al. (2005), sodium chloride (table salt) is used to represent the diffuse pollutant for its wide availability and ease of use. The grain size of the salt crystals is between 0.27 mm and 0.36 mm. At the beginning of each experiment, salt is spread uniformly on the wooden board surface. To ensure the uniformity of distribution, each board is divided into 50 (5×10) small squares and the same amount of salt (either 5 g or 2.5 g, weighted on an electronic scale) is uniformly applied within each square. Considering the fine salt grains and the tiny amount applied, it can be assumed that the salt dissolve instantly during the rainfall. In this paper, we limit our idealized study to conservative dissolved materials, but do not consider chemical reactions or the co-existence of dissolved and particle phases of the pollutant. Details on the sample collection and data recording of the runoff water and pollutant can be found in Xiao et al (2016).

4. Comparison between the analytical and experimental results

4.1. Determination of free parameters

The wash-off coefficient k and the coefficient α are the two key parameters in this study. Egodawatta et al. (2007) noted that the wash-off coefficient k is crucial in controlling the applicability of the wash-off equation. The value of k may vary with the rainfall intensity, pollutant type and the physical characteristics of the catchment (Alley, 1981; Millar, 1999). Eq. (11) indicates that the coefficient α is only related to physical characteristics of catchment but is irrelevant to the pollutant and the rainfall intensity. The value of α for each rainfall event can be determined by data fitting of the initial rising runoff process using Eq. (7). In Eq. (7), we take the measured average rainfall intensity as the value of I in each experiment. For the identical board with the same slope, we take the same value of α. The time of concentration t_c for different rainfall events can be calculated using Eq. (6). The Manning roughness coefficient n can be deduced from Eq. (11) once the value of α is determined by fitting the experimental data. Up to this point, we have obtained the values of all unknown parameters except for the wash-off coefficient k. By data fitting of the experimental results of the entire pollutant transport process, we can finally obtain the value of k.

4.2. Water runoff process

The use of rainfall and small idealized catchment simulators enables the generation of a large quantity of data in a relatively short period of time. The duration of the rainfall in our experiments is much greater than the time of concentration, so

the hydrograph is basically a S-curve. In Figs. 2 and 3, the first 10 minutes of the hydrographs are presented for clear visualization of the rising limb of the S-curve under different conditions. In the figures, S-40-1° refers to the smooth board, 40 mm/h rainfall intensity and 1° slope and similar convention applies to other notations. Figs. 2 and 3 demonstrate that the runoff processes can be predicted well by the analytical equation. Table 1 lists some quantitative information about the hydrographs, including the analytical time to plateau, analytical runoff rate at equilibrium, the mean and standard deviation of the measured flow at equilibrium, while Table 2 lists the values of α and n in different conditions. Their variation with the slope implies that the flow is not entirely hydraulically rough and thus the roughness coefficient depends on the Reynolds number of the flow. Comparison among the runoff processes in different conditions indicates that smaller rainfall intensity, milder ground slope or larger surface roughness leads to larger time of concentration. The same conclusion can be drawn from Eq. (6) and is consistent with numerous previous researches (Gottardi and Venutelli, 1993, 2008; Jaber and Mohtar, 2003; Liang et al., 2015; Xiao et al., 2016).

This study focus on the rainfall runoff over a small uniform catchment. For a large real urban catchment, there are many spatially-varied influencing factors that have an impact on the rainfall runoff process, such as buildings and vegetation. It is difficult to use a one-dimensional model to accurately simulate the response of a large real-world catchment. However, a large real-world catchment can be divided into many sub-catchments with uniform ground features and rainfall intensities. Therefore,

the rainfall-runoff process of the whole catchment can be predicted by summing up the runoff processes of the sub-catchments.

4.3. Pollutant concentration

Pollutant concentration is one of the most important indicators for evaluating the water quality, so its variation during the rainfall is studied in detail here. The comparisons between the measured and predicted pollutant concentration under different conditions are displayed in Figs. 4-7. Table 3 lists the values of k and P_c determined for different rainfall events. The experimental data for the smooth board achieve a better agreement with the analytical solution during the initial process than those for the rough board. It may be related to the limitations of the water runoff solution adopted in the analytical solution, as Govindaraju et al.(1992) noted that the kinematic wave approximation is more suitable for smooth and steep surfaces. Overall, the pollutant concentration variations are predicted satisfactorily with the present analytical model. In each condition, the pollutant concentration decreases with time, approaching to almost zero after several minutes. The pollutant concentration is highest at the beginning, corresponding to abundant material available over the catchment surface and a small flow rate. The pollutant concentration drops slowly at first, and then decreases rapidly before slowing down again towards zero. The water runoff rate is small in the initial stage and then increases rapidly to the equilibrium value. As time progresses, the amount of pollutant remaining on the surface drops. These figures show that the rainfall intensity, bed slope, surface roughness and initial

amount of pollutant all exert some degrees of influence on the concentration variations. Generally, the initial pollutant concentration increases with the increase of the rainfall intensity, increase of the bed slope, and decrease of the surface roughness. However, opposite trends are observed later on between the magnitude of the concentration and various parameters. As salt is a conservative substance, the total amount of the pollutant runoff is equal to the initial amount placed over the board.

4.4. Pollutant transport rate

The pollutant transport rate is another important indicator for quantifying the pollutant wash-off process. It is defined as the flow rate of the pollutant washed off the catchment. The measured and predicted pollutant transport rates, under different conditions, are shown in Figs. 8-11. It is evident that the variations of the pollutant transport rate under different conditions follow a similar single-peaked trend. Each curve consists of a steep rising limb at the beginning and a sharp falling limb towards the end. The pollutant runoff rate always starts from zero, and then reaches the peak, followed by the stage of declining to zero. The maximum pollutant transport rate in each condition is related to the rainfall intensity, ground slope, surface roughness, and the initial amount of pollutant. The pollutant transport rate always reaches a maximum either within or at the end of the initial rising hydrograph period, because Eq. (20) indicates the decreasing trend of the pollutant transport rate at the plateaued runoff stage. Therefore, we can formulate an expression for the maximum pollutant transport rate as follows.

Taking the derivative of Eq. (14) with respect to time and equating it to zero, we can acquire the time corresponding to the peak pollutant runoff (t_e).

$$\frac{dM_t}{dt} = \alpha BC_0 It^{\frac{2}{3}} e^{-\frac{3}{8}k\alpha L^{-1}I^{5/3}t^{8/3}} \left(\frac{\mathbf{5}}{\mathbf{3}} - k\alpha L^{-1} I^{\frac{5}{3}} t^{\frac{8}{3}} \right) = \mathbf{0}$$

$$t_e = \left(\mathbf{5}L \,/\, \left(\mathbf{3}k\alpha I^{\frac{5}{3}} \right) \right)^{3/8} \tag{22}$$

If $t_e < t_c$, then the time when reaching the maximum value is t_e, and

$$M_{\max} = BC_0 \left(\mathbf{5}LI\alpha^{\frac{3}{5}} \,/\, \left(\mathbf{3}ek \right) \right)^{5/8}$$

If $t_e \geq t_c$, then the time when reaching the maximum value is t_c, and

$$M_{\max} = AC_0 IP_c = kW_0 IP_c$$

The predicted maximum pollutant transport rates are listed in the Table 4 in the different conditions.

According to Figs. 8-11 and Table 4, the maximum pollutant transport rate increases with the rainfall intensity and ground slope, but decreases with the surface roughness. Obviously, the larger the maximum pollutant transport rate, the shorter the time taken to arrive at the maximum value. Both the analytical solution and experimental results suggest that the pollutant transport rate is proportional to the initial amount of pollutants available on the surface.

4.5. Cumulative wash-off percentage

The cumulative wash-off percentage, P_w, can be expressed as:

$$P_w = W_t / W_0 \tag{23}$$

The equation is based on the assumption that all the available pollutant is washed off

the surface after sufficient time. In practice, it is difficult to remove all of the pollutants from the surface. The final value of P_w should be less than 1 in most cases. The mathematical model for the wash-off process of particulate matters has been modified by Egodawatta et al. (2007), who suggested that a rainfall event has the capacity to mobilize only a fraction of the solids on the surface. The capacity can be quantified by a separate parameter. For dissolved pollutants, such an argument may not be suitable because the dissolved pollutants should be totally removed from the surface after an adequate duration regardless of rainfall intensity. However, only a fraction of pollutant on the surface can be collected mainly because of splashing, small leakage, etc. In order to match the experiment results and the analytical solution, we take the total collected pollutants in the end from the surface as W_0. In a similar way to the derivations in previous sections, we change the above mathematical equations into:

$$P_w = \frac{W_t}{W_0} = \frac{W_t}{F_c W_*} = \left(1 - e^{-\frac{3}{8}k\alpha L^{-1} I^{5/3} I^{8/3}}\right), \quad 0 \le t \le t_c \tag{24a}$$

$$P_w = \frac{W_t}{W_0} = \frac{W_t}{F_c W_*} = \left(1 - P_c e^{-kI(t-t_c)}\right), \quad t_c \le t \le T \tag{24b}$$

where the parameter F_c signifies the fraction of pollutant collected and W_* is the total pollutants applied in each rainfall event (125g or 250g). Figs. 12-15 illustrate the measured and predicted wash-off processes. It shows that the value of F_c in this study fluctuates within a small range from 0.87 to 0.975. The average value of F_c is 0.933, which indicates that around 93.3% of the total pollutants were collected from the surface in the end.

5. Discussions

As mentioned above, some researchers (Egodawatta et al., 2007, 2009; Sartor and Boyd , 1972) simply take the rainfall intensity to be the same as the rate of storm-water runoff per unit area when applying the exponential wash-off model. In some cases, the simplified wash-off model is found to match well with the experimental results. It should be noted that those studies focused on the cumulative wash-off only. The difference between the simplified wash-off model and the improved wash-off equations developed in this study lies in the treatment of the initial rising runoff process. The level of the difference can be measured by the difference in the cumulative wash-off percentage at time t_c. According to Eq. (3), we can acquire the formulation of the percentage of total pollutant remaining on the surface P_{c2} at time t_c. When applying the simplified wash-off model, it turns out that:

$$P_{c2} = e^{-kIt_c} = e^{-k(LI/\alpha)^{3/5}} \tag{25}$$

Comparing the above equation with Eq. (17), it is obvious that:

$$P_{c2} = P_c^{8/3} \tag{26}$$

The difference in the cumulative wash-off percentage at time t_c can thus be expressed as:

$$\Delta P = \left(1 - P_{c2}\right) - \left(1 - P_c\right) = P_c - P_c^{8/3} \tag{27}$$

Taking the derivative of Eq. (27) with respect to P_c and equating it to zero, we can acquire that the value ΔP reaches the maximum of 34.7% when P_c is about 55.5% . When the value of P_c is greater than 55.5%, ΔP decreases with increasing P_c. When the value of P_c is less than 55.5%, ΔP increases with increasing P_c. As

seen in Table 3, the value of P_c in this study varies from 28.7% to 77.5%, which means that 71.3% to 22.5% of total pollutants are washed off at the time of concentration. It suggests that the initial wash-off process is vital for dissolved pollutants. Based on the values of P_c as shown in Table 3, the values of ΔP calculated is between 25.1% and 34.7%. This analysis indicates that using the simplified wash-off model to predict such a dissolved pollutant wash-off process may cause large inaccuracies.

The value of P_c is a crucial factor in controlling the applicability of the simplified wash-off model. According to Eq. (17), the value of P_c is related to k, α and the maximum unit-width discharge (LI). Comparing the exponents of each factor, it can be seen that the wash-off coefficient k is the dominant factor. In this study, k varies from 0.63 to 1.93 mm^{-1}. However, the values of k observed for particulate pollutants on road and roof surfaces are 8×10^{-4} mm^{-1} and 9.33×10^{-3} mm^{-1} respectively (Egodawatta et al., 2007, 2009), which are significantly smaller than those in this study. It can be mainly attributed to the pollutant type and catchment properties, such as surface roughness and slope. Using the value of k observed for road and roof surfaces (Egodawatta et al., 2007, 2009) while keeping the other parameters in this study unchanged, we can calculate that the values of P_c for road surface and roof surface are greater than 99.9% and 98.9%, respectively. Furthermore, the maximum ΔP on road and roof surface are 0.15% and 1.72%, respectively. Hence, the difference between the simplified wash-off model and the newly-proposed wash-off equations becomes very small when predicting the particulate pollutant

wash-off process. This may be the reason why previous researchers found that the simplified wash-off model matched with their experimental results well.

During the initial stage of the rainfall-runoff process, the runoff rate is small and the particulate matter is not easy to be mobilized, thus only a very small amount of pollutant is washed-off at the initial stage. On the contrary, the dissolved pollutant is easier to be washed off and a significant proportion is washed off at the initial stage. Therefore, it is much more appropriate to simulate the wash-off process of dissolved pollutants using the amended wash-off equations developed in this study.

6. Conclusions

The mathematical wash-off equations for water and dissolved pollutants over small impervious catchments have been presented in this study. Through these wash-off equations, the variations of the pollutant concentration and pollutant transport rate are derived. To verify these equations, a series of laboratory experiments have been conducted. Our results show that the pollutant concentration decreases with time and its magnitude depends on the rainfall intensity, surface roughness, bed slope and initial amount of pollutant on the surface. The variation of the pollutant transport rate with time consists of an initial steep-rising stage and a subsequent sharp-decreasing stage. The larger the maximum pollutant transport rate, the shorter the time to reach the maximum value. Comparison of measured and analytical results shows that the pollutant concentration and the pollutant transport rate can be correctly described with the new wash-off equations developed in this study. In addition, we

illustrated that the degree of difference between the previous simplified wash-off model and newly-developed wash-off model depends on the value of P_c. The wash-off coefficient k is the dominant factor influencing P_c. Our analysis confirms that the initial wash-off process is crucial for dissolved pollutants, although it might not be important for particulate pollutants.

This study focuses on the water and pollutant runoff over small-scale, uniform-sloped and impervious surfaces. It is further assumed that the rainfall and the initial conservative pollutant distribution are uniform over the surface. We investigate the fundamental principles of the diffuse pollutant wash-off in this simple idealized scenario. Upscaling is a main challenge in hydrological analyses. A practical catchment is much more complicated with spatially and temporally varied rainfall intensity and ground features, but it can be divided into many small sub-catchments. In each sub-catchment, the ground slope can be assumed constant and the rainfall can be assumed uniform. The present study is expected to be useful for specifying the pollutant transport process in the sub-catchments, which can then be combined to construct the response of the entire catchment. Such a standard hydrological approach will encounter an extremely large number of free parameters, making it difficult for model calibration and verification. The advancement in modern surveying technology will partly ease this problem by feeding the model with large volume of accurate field-surveyed data.

Acknowledgements

This work was financially supported by the Ministry of Education and State Administration of Foreign Experts Affairs 111 Project (B17015), the Special Funds of the National Natural Science Foundation of China (41323001), the Chinese Academy of Engineering (2015-ZD-07-04-01) and the National Key Research and Development Program of China (2016YFC0402605).

References:

Alley, W.M., (1981). Estimation of impervious-area wash-off parameters. Water Resources Research. 17, 1161-1166.

Brezonik, P.L., Stadelmann, T.H., (2002). Analysis and predictive models of stormwater runoff volumes, loads, and pollutant concentrations from watersheds in the Twin Cities metropolitan area, Minnesota, USA. Water Research. 36, 1743-1757.

Charbeneau, RJ., Barrett, ME., (1998). Evaluation of methods for estimating stormwater pollutant loads. Water Environment Federation. 70, 1295-1302.

Deletic, A., Ashley, R., Rest, D., (2000). Modelling input of fine granular sediment into drainage systems via gully-pots. Water Research. 34, 3836-3844.

Deng, Z., de Lima, J.L.M.P., Singh, V.P., (2005). Transport rate-based model for overland flow and solute transport: Parameter estimation and process simulation. Journal of Hydrology. 315, 220-235.

Egodawatta, P., Thomas, E., Goonetilleke, A., (2007). Mathematical interpretation of pollutant wash-off from urban road surfaces using simulated rainfall. Water Research. 41, 3025-3031.

Egodawatta, P., Thomas, E., Goonetilleke, A., (2009). Understanding the physical processes of pollutant build-up and wash-off on roof surfaces. Science of the total environment. 407, 1834-1841.

Gottardi, G., Venutelli, M., (1993). A control-volume finite-element model for two-dimensional overland flow. Advances in Water Resources. 16, 277-284.

Gottardi, G., Venutelli, M., (2008). An accurate time integration method for simplified overland flow models. Advances in Water Resources. 31, 173-180.

Goonetilleke, A., Thomas, E., Ginn, S., Gilbert, D., (2005). Understanding the role of land use in urban stormwater quality management. Journal of Environmental Management. 74, 31-42.

Govindaraju, Rao.S. Kavvas, M.L., Tayfur , G., (1992). A simplified model for two-dimensional overland flows. Advances in Water Resources. 15, 133-141.

Hou, J., Bian, L., Li, T., (2013). Characteristics and sources of polycyclic aromatic hydrocarbons in impervious surface run-off in an urban area in Shanghai, China. Journal of Zhejiang University-Science A: Applied Physics and Engineering. 14, 751-759.

Irish, LB., Barrett, ME., Malina, JF., Charbeneau, RJ., (1998). Use of regression models for analyzing highway storm-water loads. Journal of Environmental Engineering. 124, 987-993.

Jaber, F.H., Mohtar, R.H., (2003). Stability and accuracy of two-dimensional kinematic wave overland flow modeling. Advances in Water Resources. 26, 1189-1198.

Kim, L., Kayhanian, M., Zoh, K., Stenstrom, M.K., (2005). Modeling of highway stormwater runoff. Science of the Total Environment. 348, 1-18.

Lee, J.H., Bang, K.W., (2000). Characterization of urban stormwater runoff. Water Research. 34, 1773-1780.

Liang, D.F., Ilhan Özgen, Reinhard Hinkelmann, Xiao, Y., Jack M. Chen., (2015). Shallow water simulation of overland flows in idealised catchments. Environmental Earth Sciences. 74, 7307-7318.

Metcalf, Eddy Inc, (1971). Storm Water Management Model, volume 1: final report, Environmental Protection Agency, Washington, D.C.

Miguntanna, N.P., Liu, A., Egodawatta, P., Goonetilleke, A., (2013). Characterising nutrients wash-off for effective urban stormwater treatment design. Journal of Environmental Management. 120, 61-67.

Millar, R.G., (1999). Analytical determination of pollutant wash-off parameters. Journal of Environmental Engineering. 125, 989-992.

Osuch-Pajdzińska, E., Zawilski, M., (1998). Model of storm sewer discharge: I Description. Journal of Environmental Engineering. 124, 593-599.

Sansalone J.J., Buchberger S.G., Al-Abed S. R. (1996). Fractionation of heavy metals in pavement runoff. The science of the total environment. 189/190: 371-378.

Sartor J. D., Boyed, .G.B., (1972). Water pollution aspects of street surface contaminants, Environmental Protection Agency, Washington, D.C.

Sheng, Y., Ying, G., Sansalone, J., (2008). Differentiation of transport for particulate and dissolved water chemistry load indices in rainfall – runoff from urban source area watersheds. Journal of Hydrology. 361, 144-158.

Stephenson D., Meadows, M.E., (1986). Kinematic Hydrology and Modelling. Elsevier Science Pubfishers, New York, USA.

Vaze, J., Chiew, F.H.S., (2002). Experimental study of pollutant accumulation on an urban road surface.

Urban Water. 4, 379-389.

Wang, S.M., He, Q., Ai, H.N., Wang, Z.T., Zhang, Q.Q., (2013). Pollutant concentrations and pollution loads in stormwater runoff from different land uses in Chongqing. Journal of Environmental Sciences. 25, 502-510.

Xiao, Y., Zhang, T.T., Liang, D.F., Jack M. Chen., (2016). Experimental study of water and dissolved pollutant runoffs on impervious surfaces. Journal of hydrodynamics. 28, 162-165.

Yao, L., Wei, W., Chen, L.D., (2016). How does imperviousness impact the urban rainfall-runoff process under various storm cases?. Ecological Indicators. 60, 893-905.

Figure and table captions

Figure 1. Experiment set-up

Photograph (a): the wooden board

Photograph (b): the rainfall simulator, the steel flume and the plastic tent at one end of the flume was for collecting runoff water samples

Figure 2. Close-up of the initial runoff rate for smooth board

Figure 3. Close-up of the initial runoff rate for rough board

Figure 4. Measured and predicted pollutant concentration (smooth board, total salt of 250g)

Figure 5. Measured and predicted pollutant concentration (rough board, total salt of 250g)

Figure 6. Measured and predicted pollutant concentration (smooth board, total salt of 125g)

Figure 7. Measured and predicted pollutant concentration (rough board, total salt of 125g)

Figure 8. Pollutant transport rate for monitored and modeled results (smooth board, total salt of 250g)

Figure 9. Pollutant transport rate for monitored and modeled results (rough board, total salt of 250g)

Figure 10. Pollutant transport rate for monitored and modeled results (smooth board, total salt of 125g)

Figure 11. Pollutant transport rate for monitored and modeled results (rough board, total salt of 125g)

Figure 12. Observed wash-off and performance of wash-off equation (smooth board, total salt of 250g)

Figure 13. Observed wash-off and performance of wash-off equation (rough board, total salt of 250g)

Figure 14. Observed wash-off and performance of wash-off equation (smooth board, total salt of 125g)

Figure 15. Observed wash-off and performance of wash-off equation (rough board, total salt of

125g)

Table 1 Key information about the hydrographs in various experimental conditions

Table 2 Estimated values for α and n

Table 3 Estimated values for k and P_c

Table 4 Estimated values for maximum pollutant transport rate

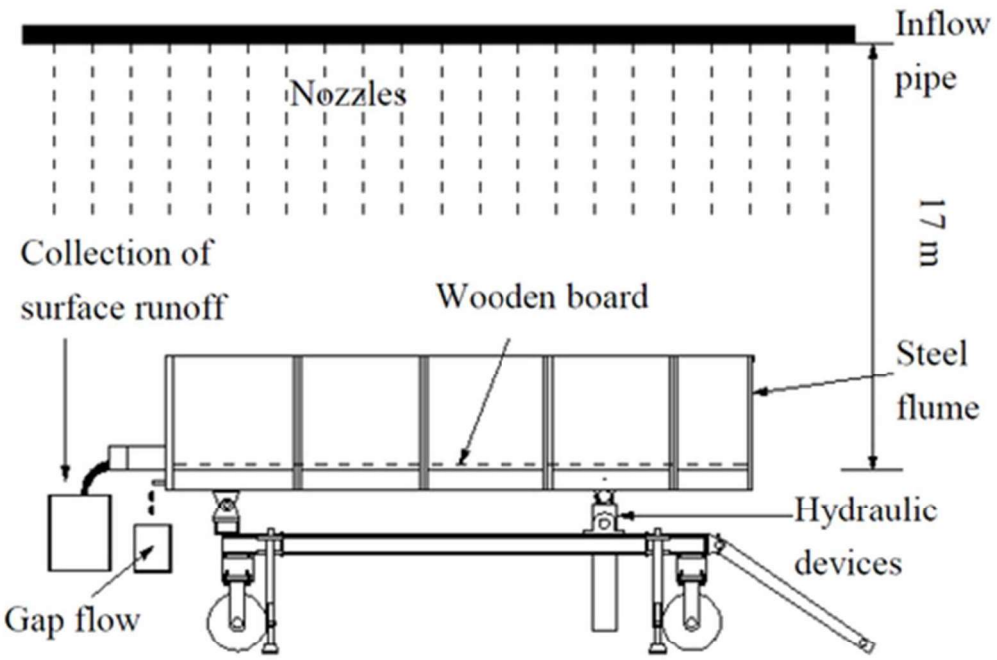

Figure 1. Experiment set-up

21x14mm (600 x 600 DPI)

Photograph (a): the wooden board

40x30mm (600 x 600 DPI)

Photograph (b): the rainfall simulator, the steel flume and the plastic tent at one end of the flume was for collecting runoff water samples

54x72mm (600 x 600 DPI)

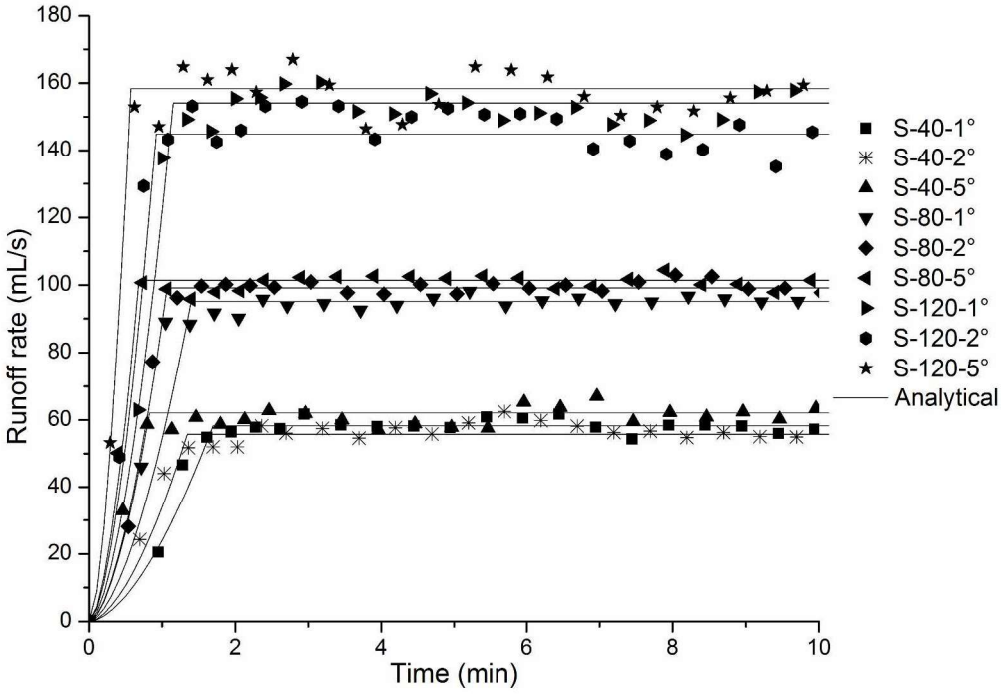

Figure 2. Close-up of the initial runoff rate for smooth board

289x203mm (300 x 300 DPI)

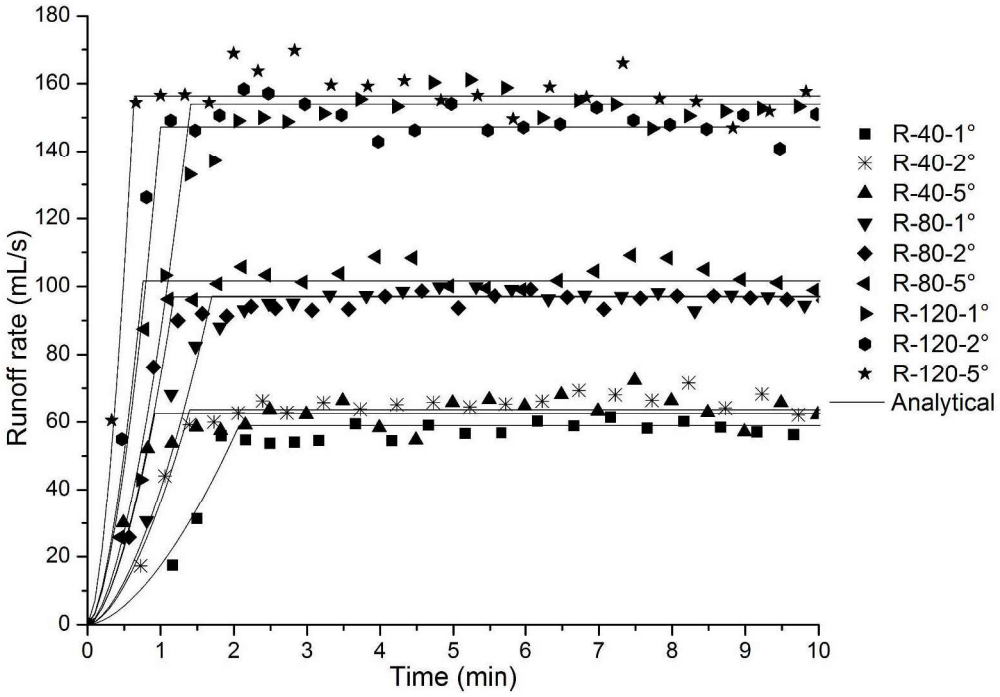

Figure 3. Close-up of the initial runoff rate for rough board

289x203mm (300 x 300 DPI)

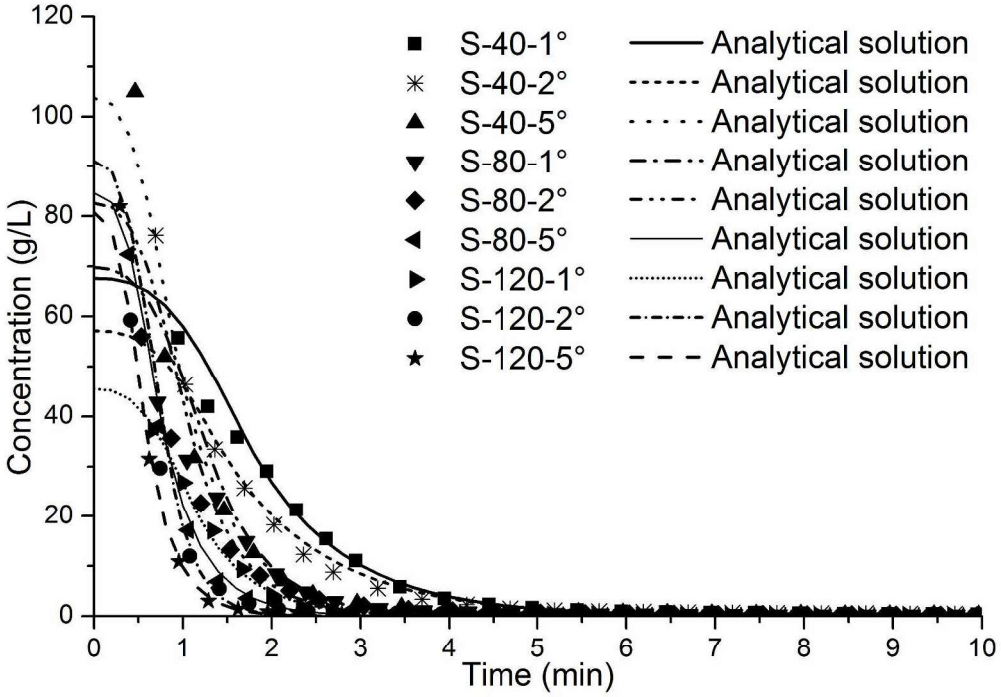

Figure 4. Measured and predicted pollutant concentration (smooth board, total salt of 250g)

289x203mm (300 x 300 DPI)

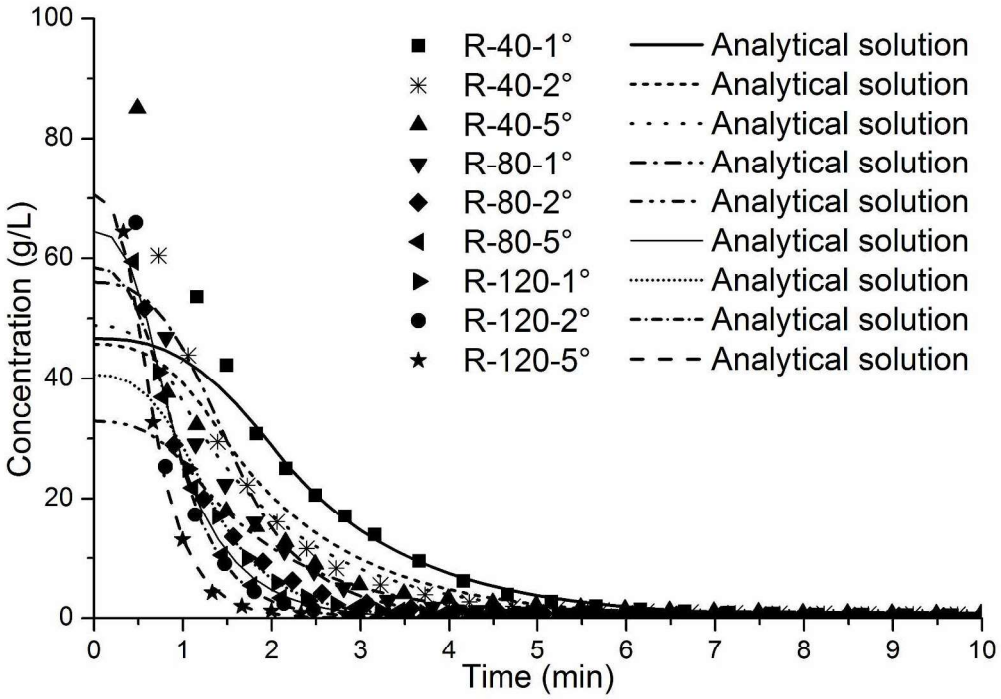

Figure 5. Measured and predicted pollutant concentration (rough board, total salt of 250g)

289x203mm (300 x 300 DPI)

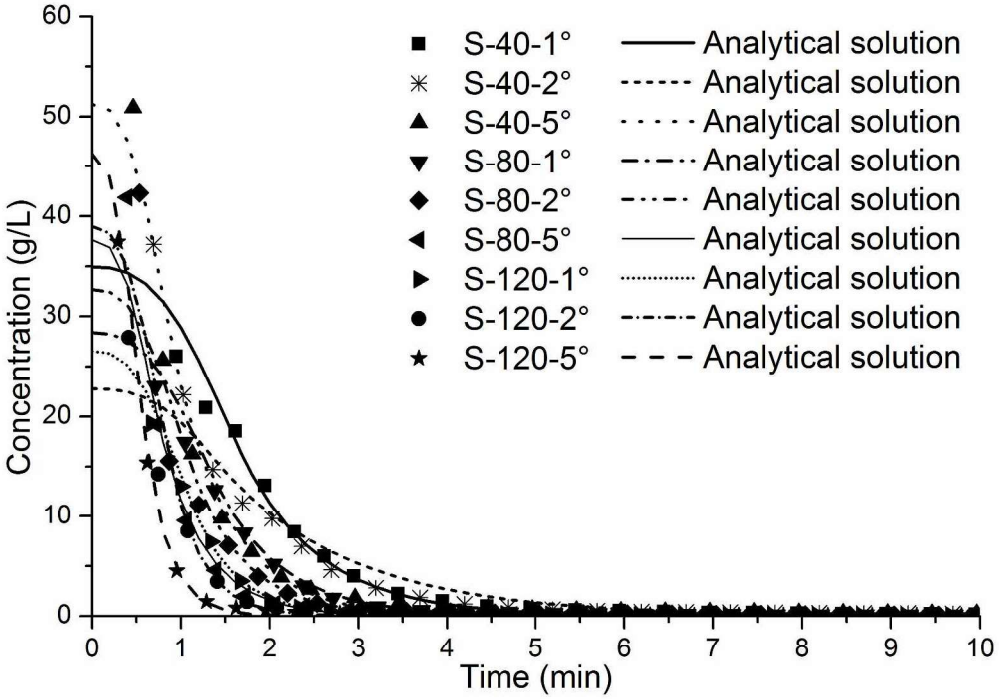

Figure 6. Measured and predicted pollutant concentration (smooth board, total salt of 125g)

289x203mm (300 x 300 DPI)

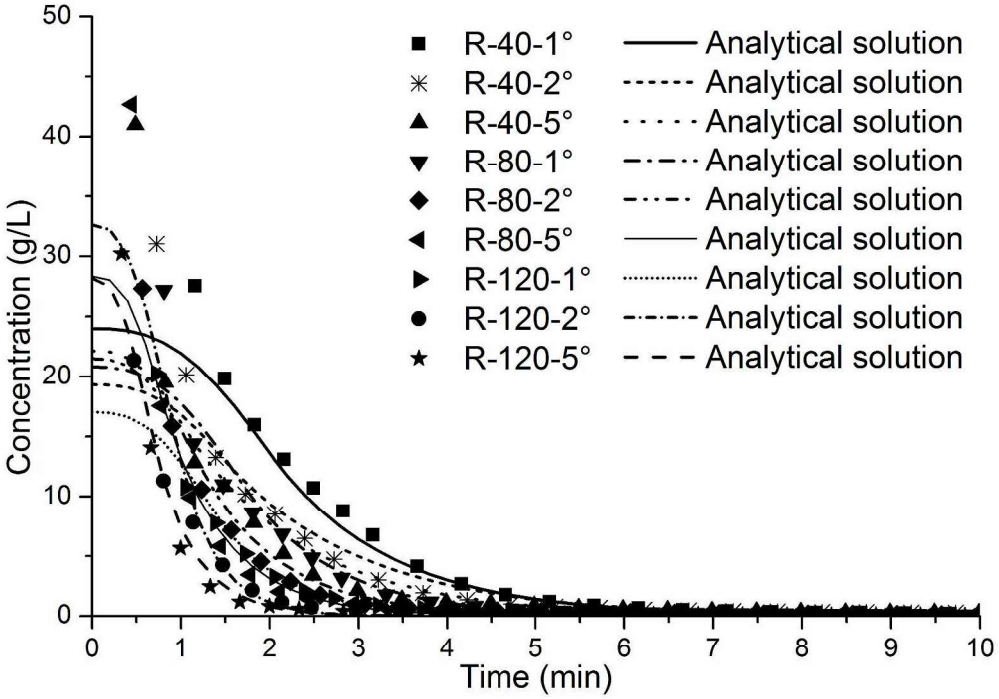

Figure 7. Measured and predicted pollutant concentration (rough board, total salt of 125g)

289x203mm (300 x 300 DPI)

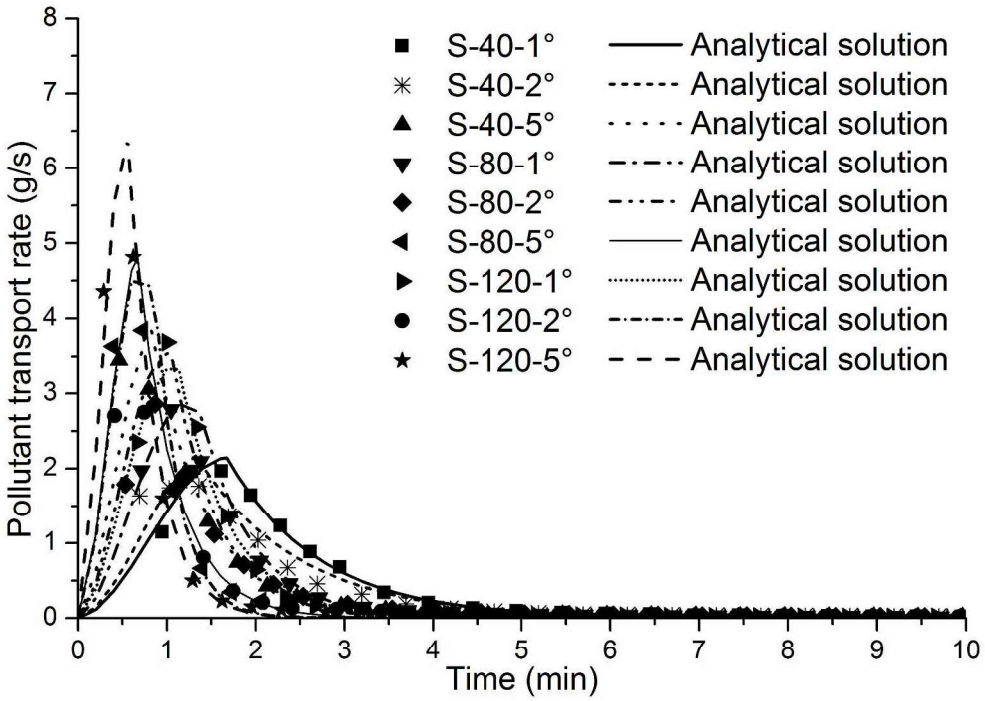

Figure 8. Pollutant transport rate for monitored and modeled results (smooth board, total salt of 250g)

289x203mm (300 x 300 DPI)

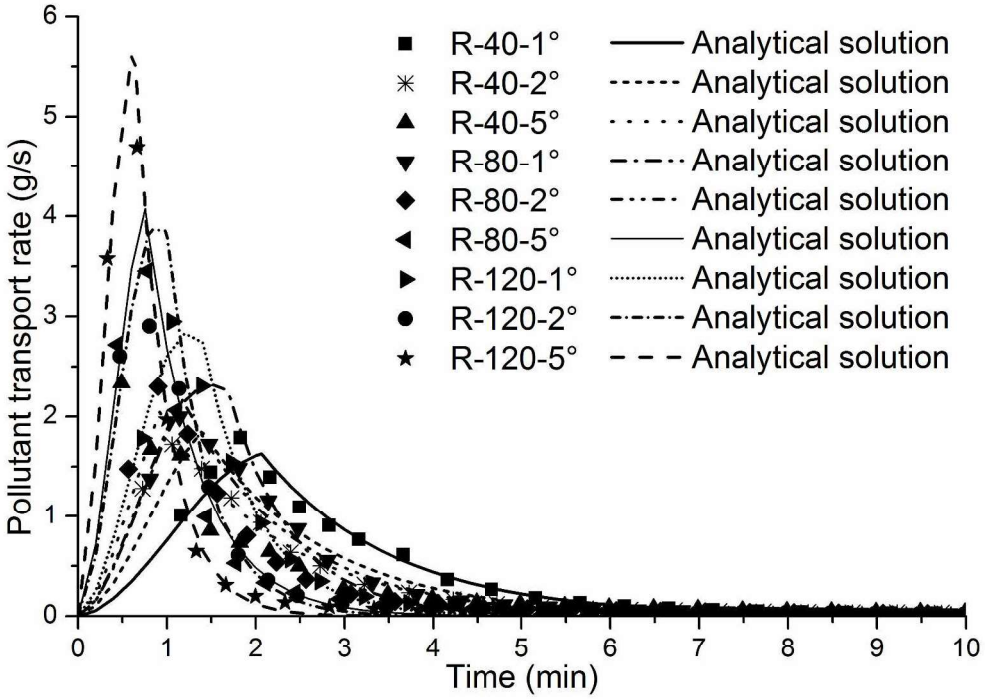

Figure 9. Pollutant transport rate for monitored and modeled results (rough board, total salt of 250g)

289x203mm (300 x 300 DPI)

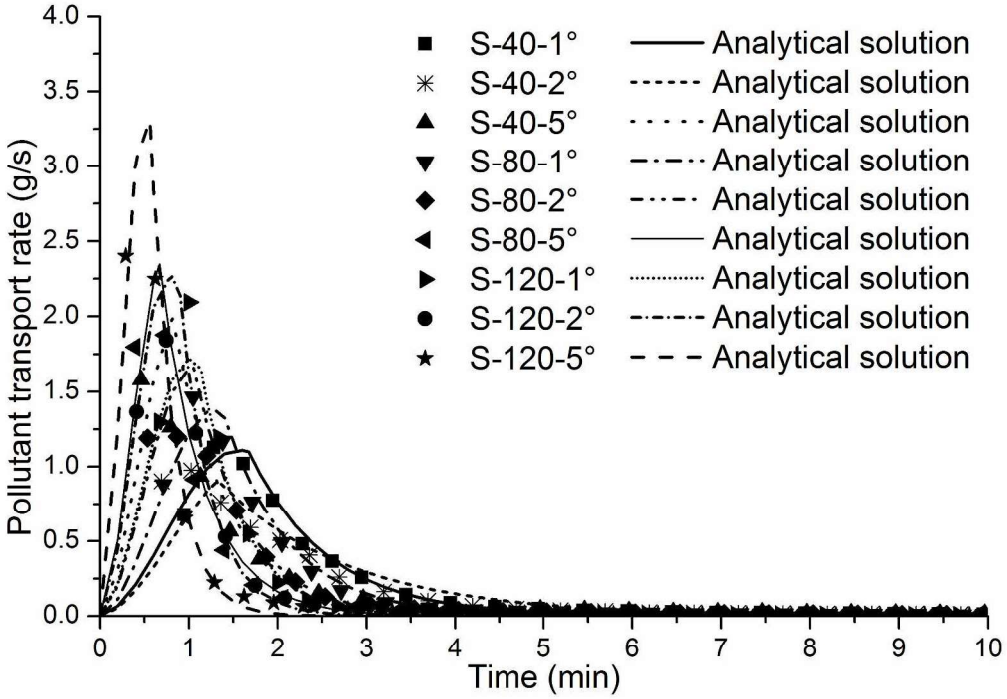

Figure 10. Pollutant transport rate for monitored and modeled results (smooth board, total salt of 125g)

289x203mm (300 x 300 DPI)

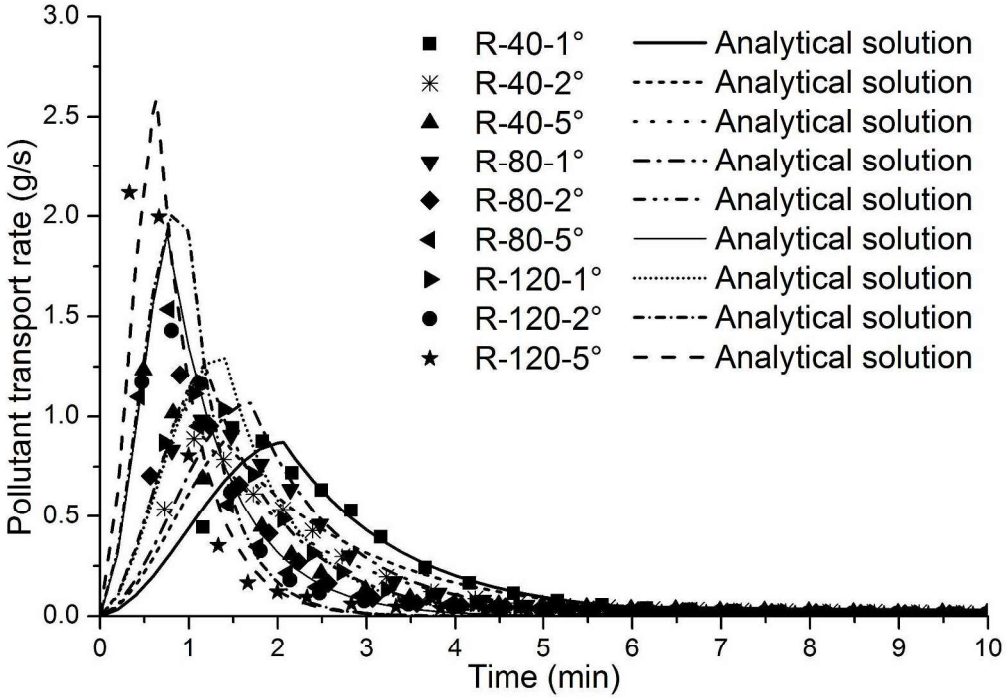

Figure 11. Pollutant transport rate for monitored and modeled results (rough board, total salt of 125g)

289x203mm (300 x 300 DPI)

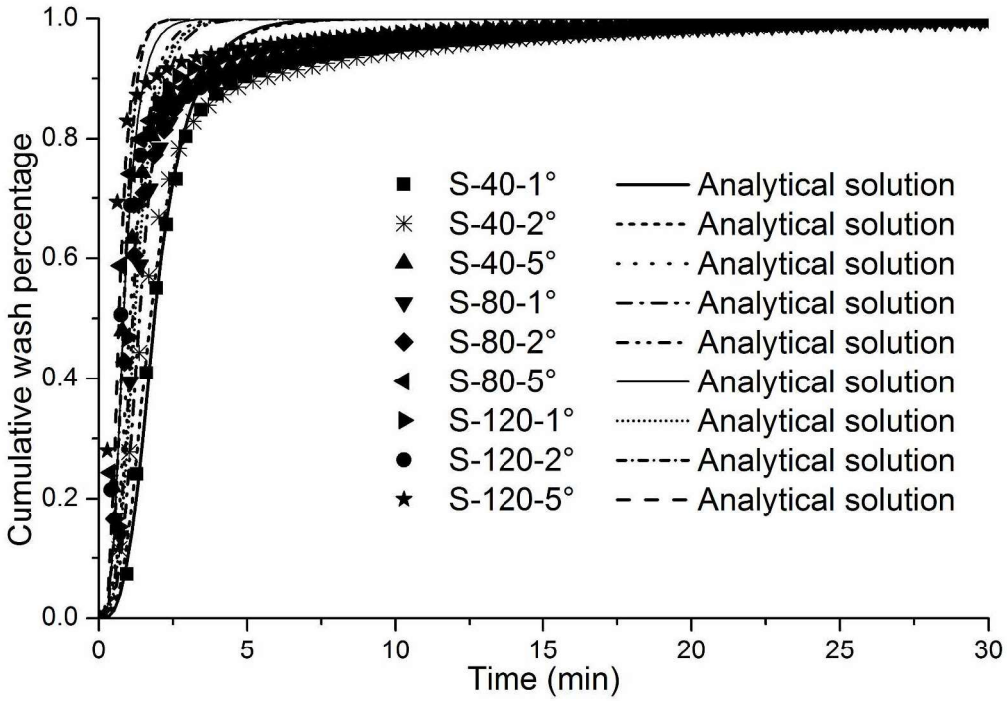

Figure 12. Observed wash-off and performance of wash-off equation (smooth board, total salt of 250g)

289x203mm (300 x 300 DPI)

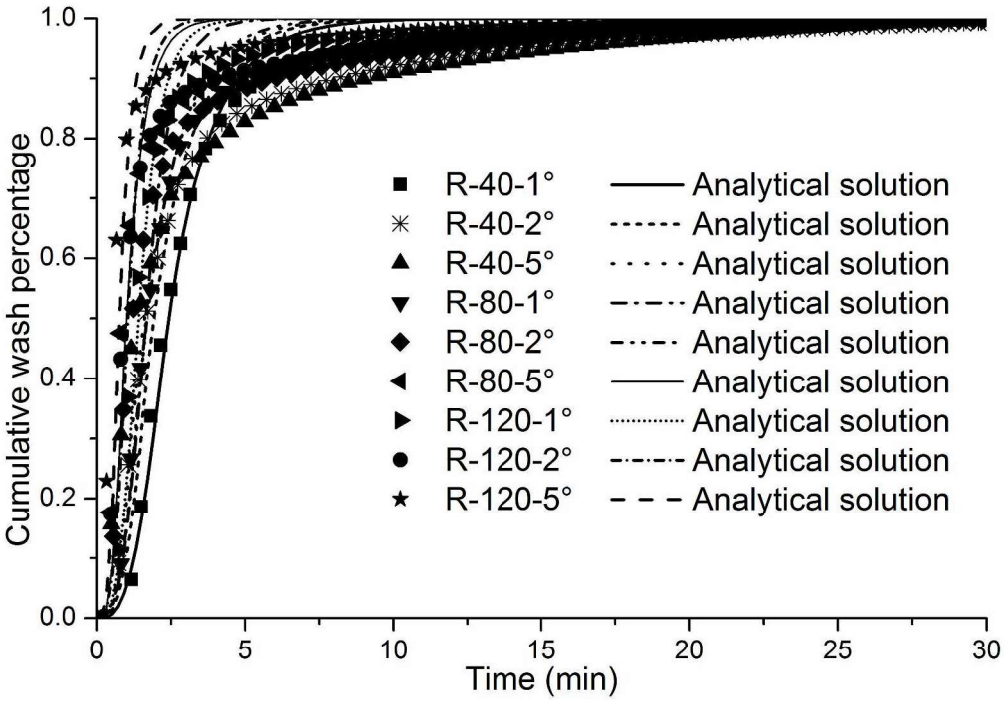

Figure 13. Observed wash-off and performance of wash-off equation (rough board, total salt of 250g)

289x203mm (300 x 300 DPI)

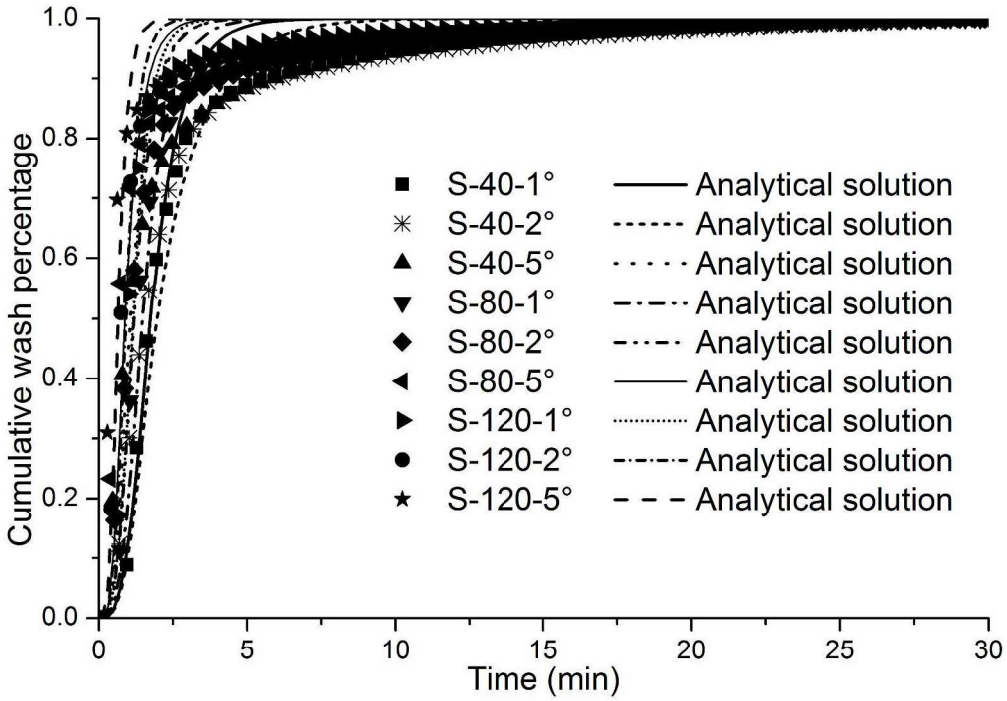

Figure 14. Observed wash-off and performance of wash-off equation (smooth board, total salt of 125g)

289x203mm (300 x 300 DPI)

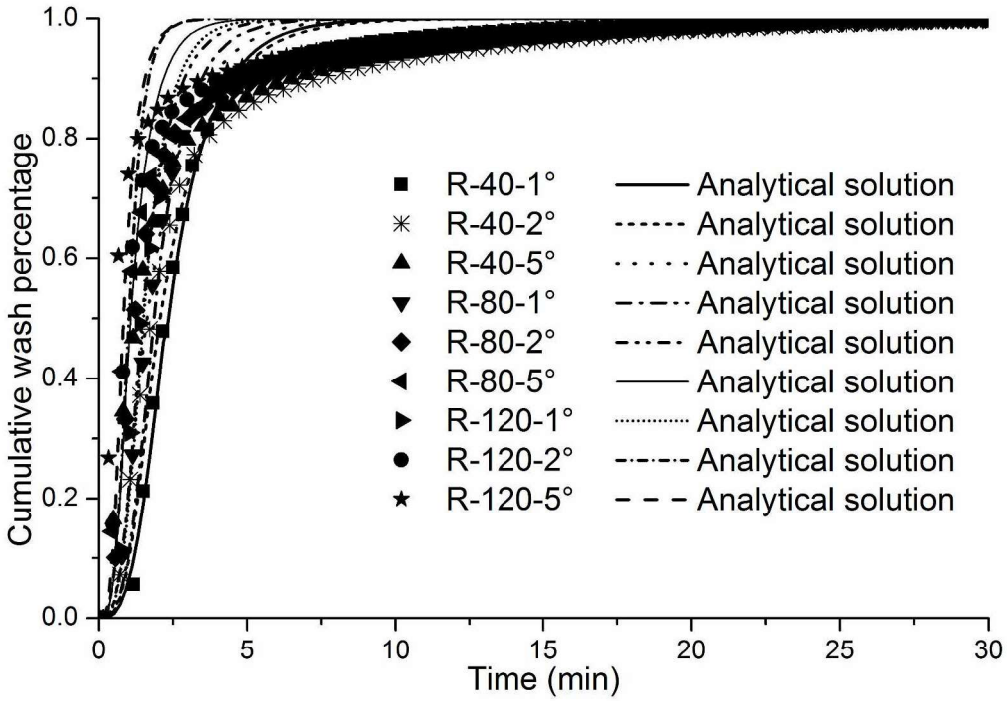

Figure 15. Observed wash-off and performance of wash-off equation (rough board, total salt of 125g)

289x203mm (300 x 300 DPI)

Table 1 Key information about the hydrographs in various experimental conditions

Board	Parameters	Rainfall intensity - Catchment slope								
		40-1	40-2	40-5	80-1	80-2	80-5	120-1	120-2	120-5
S	Predicted time to plateau (min)	1.69	1.50	0.99	1.21	0.99	0.69	1.06	0.69	0.54
	Analytical runoff rate at plateau (mL/s)	58.25	55.67	62.09	95.04	99.10	101.39	154.11	144.90	158.32
	Measured mean flow rate (mL/s)	58.20	55.52	62.01	94.93	99.08	101.13	153.94	144.86	158.23
	Standard deviation (mL/s)	2.24	2.33	3.06	1.92	2.34	2.70	5.45	6.99	5.77
R	Predicted time to plateau (min)	2.2	1.44	1.31	1.48	1.45	0.83	1.24	0.9	0.62
	Analytical runoff rate at plateau (mL/s)	58.99	63.52	62.55	97.04	96.88	101.69	154.00	147.27	156.32
	Measured mean flow rate (mL/s)	58.69	63.50	62.25	96.72	96.35	101.36	153.47	147.38	156.35
	Standard deviation (mL/s)	2.02	2.94	3.51	1.92	2.57	4.01	4.80	4.62	5.28

Table 2 Estimated values for α and n

Parameters	Test conditions					
	S-1°	S-2°	S-5°	R-1°	R-2°	R-5°
α ($m^{1/3} \cdot s^{-1}$)	2.4294	3.6969	7.7232	1.6962	3.1129	6.3127
n ($s \cdot m^{-1/3}$)	0.054	0.051	0.038	0.078	0.060	0.047

Table 3 Estimated values for k and P_c

Board	W_0 (g)	Parameters	Rainfall intensity - Slope								
			40-1	40-2	40-5	80-1	80-2	80-5	120-1	120-2	120-5
S	250	k (mm^{-1})	1.22	1.11	1.93	1.32	1.53	1.66	0.83	1.83	1.51
		P_c (%)	54.4	65.1	60.5	41.2	45.4	56.1	47.4	28.7	50.2
	125	k (mm^{-1})	1.31	0.89	1.86	1.03	1.25	1.43	1.01	1.45	1.74
		P_c (%)	50.1	71.4	61.3	49.5	51.2	60.5	40.9	37.8	45.1
R	250	k (mm^{-1})	0.84	1.37	0.96	1.05	0.63	1.22	0.75	1.07	1.32
		P_c (%)	59.1	67.9	76.6	41.4	69.4	61.6	42.8	44.2	51.1
	125	k (mm^{-1})	0.86	0.88	0.86	0.75	0.85	1.04	0.64	1.21	1.04
		P_c (%)	56.7	71.6	77.5	52.9	60.7	66.4	49.1	40.1	58.8

Table 4 Estimated values for maximum pollutant transport rate

Board	W_0 (g)	Parameters	Rainfall intensity - Slope								
			40-1	40-2	40-5	80-1	80-2	80-5	120-1	120-2	120-5
S	250	t_e (min)	1.69	1.50	0.99	1.21	0.99	0.69	1.06	0.69	0.54
		t_c (min)	1.67	1.33	0.82	1.38	1.05	0.67	1.13	0.90	0.56
		M_{max} (g/s)	2.15	2.16	2.88	2.85	3.54	4.81	3.33	3.86	6.41
	125	t_e (min)	1.56	1.67	0.89	1.30	1.03	0.72	1.00	0.77	0.51
		t_c (min)	1.67	1.33	0.82	1.38	1.05	0.67	1.13	0.90	0.56
		M_{max} (g/s)	1.11	0.91	1.98	1.38	1.66	2.34	1.64	2.13	3.31
R	250	t_e (min)	2.20	1.44	1.31	1.48	1.45	0.83	1.24	0.90	0.62
		t_c (min)	2.07	1.39	0.92	1.69	1.18	0.76	1.41	1.00	0.64
		M_{max} (g/s)	1.63	1.88	2.13	2.34	2.18	4.07	2.75	3.87	5.60
	125	t_e (min)	2.08	1.64	1.29	1.68	1.28	0.89	1.34	0.86	0.68
		t_c (min)	2.07	1.39	0.92	1.69	1.18	0.76	1.41	1.00	0.64
		M_{max} (g/s)	0.87	0.88	1.07	1.07	1.26	1.91	1.30	2.03	2.59